AJNR

Vascular Wall Imaging of Unruptured Cerebral Aneurysms with a Hybrid of Opposite-Contrast MR Angiography

T. Matsushige, Y. Akiyama, T. Okazaki, K. Shinagawa, N. Ichinose, K. Awai and K. Kurisu

AJNR Am J Neuroradiol 2015, 36 (8) 1507-1511
doi: https://doi.org/10.3174/ajnr.A4318
http://www.ajnr.org/content/36/8/1507

Vascular Wall Imaging of Unruptured Cerebral Aneurysms with a Hybrid of Opposite-Contrast MR Angiography

T. Matsushige, Y. Akiyama, T. Okazaki, K. Shinagawa, N. Ichinose, K. Awai, and K. Kurisu

ABSTRACT

BACKGROUND AND PURPOSE: Inflammation and degeneration of the intracranial saccular aneurysm wall play a major role in aneurysm formation, development and subsequent rupture. The aim of this study was to characterize the walls of unruptured intracranial aneurysms by using a hybrid of opposite-contrast MRA at 3T.

MATERIALS AND METHODS: Fourteen consecutive patients with 17 unruptured intracranial aneurysms who initially underwent clipping surgery were prospectively evaluated. All aneurysms were scanned preoperatively by using a hybrid of opposite-contrast MRA in 3T high-resolution MR imaging. We classified intraoperative findings of atherosclerotic plaques in the aneurysms into 3 grades: grade A (major plaques), grade B (minor plaques), and grade C (no plaques). The contrast ratio of the high-intensity area was also measured relative to the background low-intensity area inside the carotid artery.

RESULTS: Findings from preoperative plaque imaging of the aneurysm corresponded to the intraoperative findings in 15 of 16 aneurysms (excluding 1 that was impossible to visualize in its entirety due to anatomic reasons). Overall sensitivity and specificity of the hybrid of opposite-contrast MRA were 88.9% and 100%, respectively. During the operation, 4 aneurysms were classified as grade A; 5, as grade B; and 7, as grade C. The means of the contrast ratio for grades A, B, and C were 0.72 ± 0.03, 0.34 ± 0.30, and −0.02 ± 0.09, respectively.

CONCLUSIONS: The hybrid of opposite-contrast MRA can detect visible atherosclerotic plaques in the unruptured aneurysm wall, and the contrast ratio in intracranial aneurysms correlated with their presence and extent. A study including a larger series is needed to validate the diagnostic potential of this imaging technique.

ABBREVIATIONS: AcomA = anterior communicating artery; FSBB = flow-sensitive black-blood; HOP-MRA = hybrid of opposite-contrast MR angiography; WVCR = wall-vessel lumen contrast ratio

Intracranial aneurysms are common vascular lesions, often consisting of a saccular dilation of a cerebral artery vessel. The prevalence of intracranial aneurysms in the general population is estimated between 2.5% and 5%.[1,2] Aneurysmal rupture occurs with a 1% risk per year, depending on the size, location, and morphometry of the aneurysm, and leads to subarachnoid hemorrhage with associated high morbidity and mortality rates.[1,2] Intracranial aneurysms with an estimated high risk of rupture undergo management via a surgical or endovascular approach, depending on the specific risks of treatment.[3,4] Therefore, it is important to accurately assess the risk of aneurysmal rupture.

The pathogenesis of intracranial aneurysms and their natural history are not well-understood. Histopathologic studies have shown that the infiltration of inflammatory cells and the degeneration of the aneurysm wall with atherosclerosis correlates with the formation, development, and rupture risk of cerebral aneurysms.[5-9] However, characterization of the aneurysm wall is limited by imaging data quality and the need to harvest surgical specimens.

In this regard, the characteristics of high-field-strength MR imaging, which has a favorable SNR and changes in relaxation time and susceptibility, can depict the intracranial vessel walls and their pathologies, including small vessels with atherosclerosis.[10,11]

The hybrid of opposite-contrast MR angiography (HOP-MRA) used in this study is a modern technique that combines the advantages of 3D TOF MRA and flow-sensitive black-blood (FSBB) MRA.[12] The clinical efficacy of this technique was established to improve the visualization of peripheral vessels.[13,14] The-

Received September 17, 2014; accepted after revision January 9, 2015.

From the Department of Neurosurgery (T.M., T.O., K.S., N.I., K.K.), Graduate School of Biomedical and Health Sciences, Hiroshima University, Hiroshima, Japan; Department of Neurosurgery (T.M.), University Hospital Essen, Essen, Germany; and Department of Diagnostic Radiology (Y.A., K.A.), Institute of Biomedical and Health Sciences, Hiroshima University, Hiroshima, Japan.

Paper previously presented at: Annual Meeting of Radiological Society of North America, November 30–December 5, 2014; Chicago, Illinois.

Please address correspondence to Toshinori Matsushige, MD, PhD, Department of Neurosurgery, University Hospital Essen, Hufelandstr 55, 45147, Essen, Germany; e-mail: teruteru728@hiroshima-u.ac.jp

http://dx.doi.org/10.3174/ajnr.A4318

oretically, tissue with shorter T1 and T2* introduces high signal in FSBB of HOP-MRA, which demonstrates atherosclerotic plaques, including fat, as high-signal-intensity areas and demonstrates the blood space as low-signal-intensity areas in intracranial aneurysms.[12] The strength of this technique is the dual-echo 3D gradient-echo sequence, which enables a shorter imaging time and minimization of misregistration. The present study investigated the utility of HOP-MRA at 3T for the characterization of visible atherosclerotic plaques in intracranial aneurysms by using subtraction between TOF and FSBB imaging.

MATERIALS AND METHODS

Study Design

This study was approved by an institutional review committee, and the subjects gave informed consent to participate. It prospectively evaluated the diagnostic feasibility of delineating the aneurysm wall by using HOP-MRA at 3T in comparison with intraoperative findings of the aneurysm. Inclusion criteria were the following: 1) patients undergoing elective clipping surgery, 2) 18–80 years of age, and 3) the ability to give informed consent. Exclusion criteria were the following: 1) presence of cardiac pacemaker or any other electronic implants, 2) pregnancy or breast feeding, and 3) claustrophobia.

Preoperative Image Evaluation

Preoperative assessment of aneurysms in our institution includes routine cerebral DSA, CTA, and MR imaging. Calcification of the aneurysm was assessed by using CTA with sections of 1-mm thickness with a 0.5-mm overlap. The morphology, location, and size of the aneurysm were assessed by 3D rotational DSA by the operating neurosurgeon with 16 years of experience (T.O.). Additionally the presence of high signal intensity in the aneurysm wall was evaluated on multiplanar reconstruction (transverse, coronal, and sagittal) of HOP-MRA at 3T by a second neurosurgeon (T.M.) before the operation.

Intraoperative Assessment

The aneurysm was completely exposed via the trans-Sylvian or interhemispheric approach by craniotomy. Intraoperative evaluation of the aneurysm wall was performed in consensus by both neurosurgeons. In addition, a third neurosurgeon with 10 years of experience (K.S.), who was blinded to preoperative MR imaging data, evaluated the microscopic findings on all aneurysms by operative video. Microscopic surgical findings of the aneurysm wall were defined by visible atherosclerotic changes (yellowish) and classified into 3 grades by the neurosurgeons as grade A (major plaques), grade B (minor plaques), and grade C (no plaques).

HOP-MRA Sequence

All images were acquired on a commercially available 3T MR imaging scanner (Vantage Titan 3T; Toshiba Medical Systems, Tokyo, Japan) equipped with a 6-channel head coil. For HOP-MRA, we used a 3D gradient-echo, double-echo sequence. TEs were chosen for TOF-contrast with the first echo and FSBB contrast with the second echo. The 2 original images were subtracted and displayed by maximum intensity projection. The scan parameters were the following: acquisition time, 7:00 min; TR, 21 ms; TE 1, 3.3 ms (TOF); TE 2, 13.9 ms (FSBB); flow-dephasing gradient ($b = 0.3$ s/mm^2); flip angle, 20°; field of view, 240 mm; section thickness, 1 mm; number of partitions, 60; matrix, 192 × 256; and NEX, 2.

Image Evaluation

A radiologic technician (19 years of experience) measured the mean signal intensity of the highest intensity area in the aneurysm wall compared with the background low-intensity area inside the ipsilateral carotid artery. Imaging data were transferred to an Advantage Workstation (Version 3.1; GE Healthcare, Milwaukee, Wisconsin) with Virtual Place Office (Azemoto, Tokyo, Japan) software to perform postprocessing. Diameters for the ROIs in the aneurysm wall were 2 mm^2 without including voxels from adjacent structures. The ROI in the carotid artery was thought to be suitable for referring intensity very close to that of most aneurysms and was placed in the center of the ipsilateral carotid artery amounting to 2 mm^2. The wall-vessel lumen contrast ratio (WVCR = $\text{Signal}_{\text{wall}} - \text{Signal}_{\text{vessel lumen}}/\text{Signal}_{\text{wall}} + \text{Signal}_{\text{vessel lumen}}$) was also assessed.

Statistical analyses were performed by using the JMP statistical package (Version 10; SAS Institute, Cary, North Carolina). To compare differences between 2 groups, we used the Fisher exact test for categoric factors between 2 groups and the Mann-Whitney *U* test for quantitative variables. Statistical significance was indicated by $P < .05$.

RESULTS

All patients tolerated the examination well, and this prospective study included 14 patients (6 men, 8 women; median age, 60 years; age range, 24–76 years) with 17 aneurysms in total. Patient demographics including vascular atherosclerotic risk factors such as sex, age, hypertension, dyslipidemia, diabetes mellitus, and cigarette smoking are summarized in the Table. The evaluation by DSA showed that all aneurysms were located in the anterior circulation (ICA, $n = 3$; anterior cerebral artery, $n = 8$; and MCA, $n = 6$). The median maximum diameter of the aneurysms was 5.4 mm (range, 2.8–14.1 mm). There were no aneurysms with calcification on thin-section CTA.

The interobserver assessment between 2 neurosurgeons in consensus during the operation and another neurosurgeon was identical. Of 17 aneurysms, we delineated 9 aneurysms with thickened walls corresponding to high signal intensity. During the operation, 4 aneurysms were classified as grade A; 5, as grade B; and 7, as grade C. One aneurysm could not be completely characterized because it arose from the ICA terminal with posterior projection (case 5).

If we excluded this aneurysm, which was anatomically impossible to assess, 15 of 16 (93.8%) aneurysms showed excellent correlation between the surgical overview and the presence of high signal in the aneurysm wall. Overall sensitivity of HOP-MRA was 88.9%, and specificity was 100%. There was no correlation between the presence of atherosclerosis and vascular atherosclerotic risk factors: sex ($P = .70$), age ($P = .83$), hypertension ($P = .62$), dyslipidemia ($P = .64$), diabetes mellitus ($P = 1.00$), and cigarette smoking ($P = .64$). However, there was a statistically significant difference between the presence of atherosclerosis and aneurysm size ($P = .03$). The mean WVCR of the aneurysm wall with atherosclerotic plaques (grades A and B) was significantly higher than that in the aneurysm wall without plaques (grade C) ($P =$

Patient demographics and findings

Case No.	Aneurysm No.	Patients: Sex	Patients: Age (yr)	Aneurysms: Location	Aneurysms: Maximum Size (mm)	Aneurysms: Intraoperative Plaque Findings[a]	Aneurysm Wall Findings at HOP-MRA: High Signal Intensity	Aneurysm Wall Findings at HOP-MRA: WVCR[b]	Atherosclerotic Risk Factors: HT	DL	DM	CS
1	1	M	24	ICA Ach	4.2	A	+	0.73	+	−	−	−
2	2	M	35	ACA (A1)	2.8	C	−	−0.02	+	−	−	+
3	3	M	69	MCA	6.1	C	−	−0.22	−	+	−	+
4	4	M	76	MCA	14.1	A	+	0.70	+	−	−	+
5	5	F	71	ICA PcomA	5.9	C	−	0.01	−	+	−	+
	6	F	71	ICA terminal	3.5	NA[c]	+	0.64	−	+	−	+
6	7	F	53	dACA	7.2	A	+	0.68	+	+	−	+
	8	F	53	dACA	6.7	B	+	0.62	+	+	−	+
	9	F	53	AcomA	4.2	C	−	0.02	+	+	+	+
7	10	F	63	MCA	5.4	B	+	0.04	+	+	−	−
8	11	F	70	MCA	5.1	B	+	0.44	−	+	−	−
9	12	M	60	AcomA	4.7	C	−	0.00	+	−	−	−
10	13	F	63	AcomA	5.0	B	−	0.02	+	+	−	−
11	14	M	61	MCA	7.2	B	+	0.60	+	−	−	+
12	15	F	73	MCA	9.6	A	+	0.75	−	−	−	−
13	16	F	55	AcomA	4.0	C	−	0.04	+	−	−	+
14	17	F	69	AcomA	5.6	C	−	0.03	−	+	−	−

Note:—Ach indicates anterior choroidal artery; PcomA, posterior communicating artery; ACA (A1), anterior cerebral artery (A1 segment); dACA, distal anterior cerebral artery; HT, hypertension; DL, dyslipidemia; DM, diabetes mellitus; CS, cigarette smoking; NA, not assessed due to anatomic reasons; +, present; −, absent.

[a] Intraoperative plaque assessment in the aneurysm was demonstrated as the following: grade A, major plaques; grade B, minor plaques; grade C, no plaques.

[b] WVCR indicates a high-intensity area in the aneurysm wall to the background low-intensity area inside the aneurysm.

[c] Impossible to characterize the entire aneurysm due to anatomic reasons.

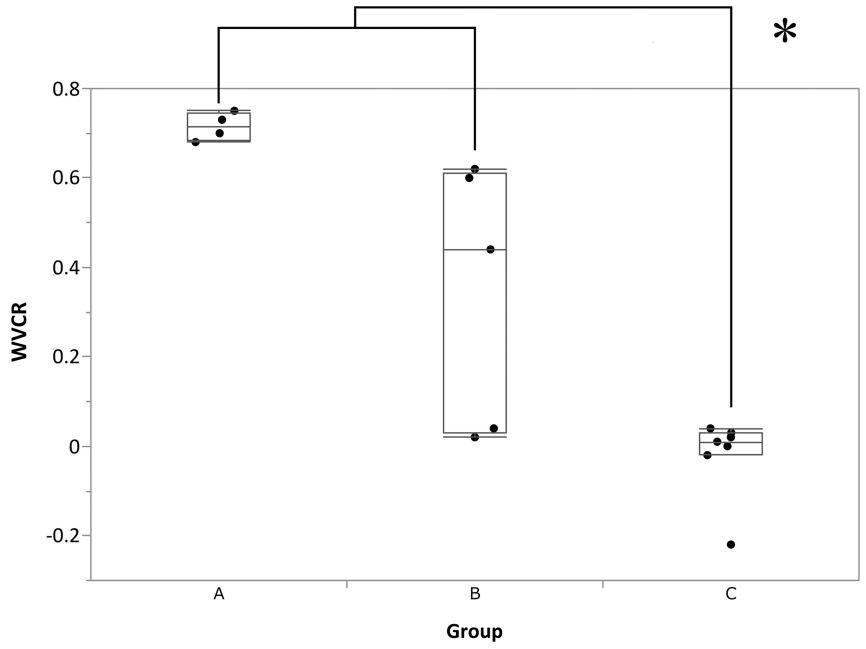

FIG 1. The distribution of WVCR in each plaque in the aneurysm wall. There is a significant difference in WVCR among A, B, and C ($P = .0011$). Group A indicates major plaques; group B, minor plaques; and group C, no plaques.

.0011). The means of the WVCRs for grades A, B, and C were 0.72 ± 0.03, 0.34 ± 0.30, and -0.02 ± 0.09, respectively. Details are illustrated in Fig 1.

Illustrative Cases

Case 1. A hypertensive 24-year-old man with a familial history of subarachnoid hemorrhage had an unruptured left ICA-anterior choroidal artery aneurysm of 4.2-mm maximum diameter (Fig 2*A-1*). Despite the patient's age, high signal intensity in the aneurysm wall was delineated by the presurgical FSBB. The lesion had a high contrast ratio (WVCR = 0.73) (Fig 2*A-2*). Atherosclerotic plaques in the aneurysm wall were evaluated as grade A intraoperatively (Fig 2*A-3*).

Case 8. A 70-year-old woman with an unruptured left MCA aneurysm of 5.1-mm maximum diameter was referred to our hospital (Fig 2*B-1*). Partial high signal intensity in the aneurysm wall was delineated by presurgical FSBB (Fig 2*B-2*). The lesion presented with mild elevation of contrast ratio (WVCR = 0.44). An intraoperative view via a trans-Sylvian approach showed the patchy atherosclerotic change on the wall, which was evaluated as grade B (Fig 2*B-3*).

Case 3. A 69-year-old man had an unruptured right MCA aneurysm of 6.1 mm maximum (Fig 2*C-1*). There was no high signal intensity in the aneurysm wall in the presurgical FSBB (Fig 2*C-2*). An intraoperative view via a trans-Sylvian approach showed no atherosclerosis in the aneurysm wall. The aneurysm wall was evaluated as grade C (Fig 2*C-3*).

Case 10. A 63-year-old woman with an unruptured anterior communicating artery (AcomA) aneurysm presented to our hospital (Fig 2*D-1*). FSBB failed to show high signal intensity that would have otherwise corresponded to atherosclerotic plaque in the aneurysm wall (Fig 2*D-2*). The actual intraoperative view showed

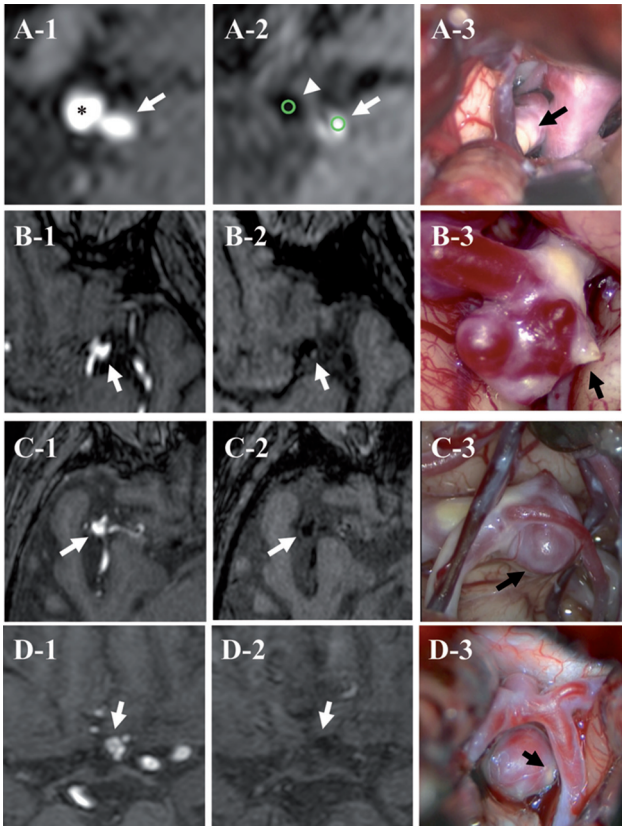

FIG 2. TOF-MRA (*first column*), FSBB (*second column*), and an intraoperative photomicrograph (*third column*) of 4 different patients with various degrees of atherosclerosis in the aneurysm wall. *A*, Left ICA–anterior choroidal artery unruptured aneurysm from case 1. TOF-MRA depicts the aneurysm (*A-1*, *arrow*) and left carotid artery (*A-1*, *asterisk*). FSBB shows high signal intensity in most of aneurysm wall with ROIs (*green circle*) in the wall (*A-2*, *arrow*) and at the center of the ipsilateral ICA for measuring the referring intensity (*A-2*, *arrowhead*). Intraoperative view showing abundant atherosclerotic plaques (grade A) in the aneurysm wall (*A-3*, *arrow*). *B*, Left MCA aneurysm from case 8. TOF-MRA shows the aneurysm (*B-1*, *arrow*). FSBB depicts focal high signal intensity in the aneurysm wall (*B-2*, *arrow*), corresponding to a patchy atherosclerotic plaque (grade B) in the intraoperative view (*B-3*, *arrow*). *C*, Right MCA aneurysm from case 3. TOF-MRA demonstrates the aneurysm (*C-1*, *arrow*). FSBB shows no high signal intensity in the wall (*C-2*, *arrow*), and the intraoperative view also shows no plaques (grade C) in the wall (*C-3*, *arrow*). *D*, Left AcomA aneurysm from case 10. TOF-MRA depicts the aneurysm (*D-1*, *arrow*), and FSBB shows no high signal intensity in the aneurysm wall (*D-2*, *arrow*). The operative view shows a small patchy atherosclerotic change on the right body of the aneurysm (*D-3*, *arrow*).

small atherosclerotic change on the right body of the aneurysm (Fig 2*D-3*).

DISCUSSION

This study showed that HOP-MRA at 3T can detect atherosclerotic plaques in the aneurysm wall preoperatively and that the WVCR in intracranial aneurysms correlated with the presence and extent of visible atherosclerotic plaques. This is the first report to show that high-resolution MR imaging, including the HOP-MRA technique at 3T, can delineate plaque in the aneurysm wall, though we found some studies on aneurysm wall imaging.[15-20]

In recent years, there is much evidence that inflammation and degeneration of the aneurysm wall play a major role in aneurysm formation, development, and rupture.[5-9] Along with elucidation of the histopathology of the aneurysm wall, it is expected vessel wall imaging will reveal biologic behavior of the aneurysm wall. Some authors reported the possibility of detecting unstable intracranial aneurysms by using contrast media, which in our opinion, corresponds to increased aneurysm wall permeability.[17,18] Aneurysm wall imaging can be performed with ultrasmall superparamagnetic particles of iron oxide (ferumoxytol) to reveal inflammation surrounding the aneurysm wall.[19] Recently, vessel wall imaging at 7T was reported to reveal variations of aneurysm wall thickness.[20] Ours is a novel study comparing the atherosclerotic changes of the aneurysm wall, which are presumably associated with one of the processes of degeneration, between HOP-MRA and the operative view.

Atherosclerotic change in the cerebral aneurysm wall is part of the pathologic degeneration underlying the development of inflammation.[5-9,21] The progression of the degeneration is considered to have a positive correlation with aneurysmal growth.[21] Although whether the presence of atherosclerosis correlates with the risk of aneurysm rupture is not yet well-known, we believe that the delineation of the aneurysm wall yields valuable information regarding intracranial cerebral aneurysms. As shown in our series, the signal intensity varied according to the degrees of atherosclerosis. The presence of high signal intensity on HOP-MRA may reflect the vulnerability of the plaque in the aneurysm wall.

In clinical practice, ischemic surgical complications are more likely if there is atherosclerotic change around the wall of the cerebral aneurysm.[22,23] It is possible that the fragile plaque migrates distally during the clipping procedure. We had a few patients who had silent ischemic lesions on diffusion-weighted imaging, as retrospectively proved by operative video. Some aneurysms that were surgically treated could not be completely observed for anatomic reasons. In such cases, preoperative imaging to determine the presence or absence of active atherosclerotic plaque around the neck of aneurysm is helpful for surgical planning and other treatment decisions.

High-resolution MR vessel wall imaging, including high-resolution black-blood imaging by presaturation pulse or a double inversion recovery black-blood sequence, yields information regarding the pathology of small cerebrovascular diseases.[10,11] Most vessel wall imaging techniques focus on steno-occlusive cerebrovascular disease with well-established atherosclerotic plaque imaging, though some imaging strategies can also yield information regarding the wall of cerebral aneurysms.[15-20] The strengths of the HOP technique include minimization of misregistration, among others. Because we performed TOF-MRA and FSBB simultaneously, we characterized the plaque clearly without the influence of pulse and flow in the aneurysm. To reduce the time and uncertain high signal by artifacts during FSBB imaging, we used a dual-echo 3D gradient-echo sequence and a high TE and b factor.

This study had several limitations. First, the comparison between the plaque imaging and the intraoperative view was subjective, though it was performed in a blinded manner by experienced neurosurgeons and radiologic technicians. Furthermore, because we routinely expose all parts of the aneurysm to mobilize it during microsurgical clipping, we were able investigate and record all these parts. Second, it is difficult to harvest a small aneurysm wall safely to compare the result of HOP-MRA and ex vivo pathologic

examination. Therefore, we could not determine why false-negative results on HOP-MRA occurred in the presence of patchy atherosclerotic plaque (case 10). We speculated that the degree of plaque containing vulnerable component might account for this phenomenon. High signal intensity in the aneurysm wall may include the presence of intraluminal thrombus, which is on the same degenerative pathway of the aneurysm wall.[6,7] Additionally, this study did not include calcified aneurysms. Vessel wall calcification is also a part of degeneration. Further study is needed to investigate whether HOP-MRA can characterize atherosclerosis with calcification and to characterize the precise spread, location, and the activity of atherosclerosis in relation to aneurysms.

Although HOP-MRA is a promising technique to determine the degree of atherosclerotic change in cerebral aneurysms, its clinical availability is limited. Although this study involved a small sample set, we believe that aneurysm wall imaging could become a standard examination to identify rupture-prone cerebral aneurysms.

CONCLUSIONS

The high signal intensity in intracranial aneurysms on HOP-MRA imaging correlated with the presence and extent of atherosclerotic plaques in the intracranial aneurysm wall.

ACKNOWLEDGMENTS

We thank Drs Ulrich Sure, Karsten H. Wrede, and Philipp Dammann of the University Hospital of Essen for their technical advice.

Disclosures: Kazuo Awai—*RELATED*: *Grant*: Toshiba Medical Systems (research grant)*; *Consulting Fee or Honorarium*: Toshiba Medical Systems (consultant); *Grants/Grants Pending*: Eizai,* Bayer,* Yakuhin*, Diichi Sankyo.* *Money paid to the institution.

REFERENCES

1. Wiebers DO, Whisnant JP, Huston J 3rd, et al. **Unruptured intracranial aneurysms: natural history, clinical outcome, and risks of surgical and endovascular treatment.** *Lancet* 2003;362:103–10
2. Morita A, Kirino T, Hashi K, et al. **The natural course of unruptured cerebral aneurysms in a Japanese cohort.** *N Engl J Med* 2012;366:2474–82
3. Naggara ON, Lecler A, Oppenheim C, et al. **Endovascular treatment of intracranial unruptured aneurysms: a systematic review of the literature on safety with emphasis on subgroup analyses.** *Radiology* 2012;263:828–35
4. Kotowski M, Naggara O, Darsaut TE, et al. **Safety and occlusion rates of surgical treatment of unruptured intracranial aneurysms: a systematic review and meta-analysis of the literature from 1990 to 2011.** *J Neurol Neurosurg Psychiatry* 2013;84:42–48
5. Kataoka K, Taneda M, Asai T, et al. **Structural fragility and inflammatory response of ruptured cerebral aneurysms: a comparative study between ruptured and unruptured cerebral aneurysms.** *Stroke* 1999;30:1396–401
6. Frosen J, Piippo A, Paetau A, et al. **Remodeling of saccular cerebral artery aneurysm wall is associated with rupture: histological analysis of 24 unruptured and 42 ruptured cases.** *Stroke* 2004;35:2287–93
7. Frosen J, Tulamo R, Paetau A, et al. **Saccular intracranial aneurysm: pathology and mechanisms.** *Acta Neuropathol* 2012;123:773–86
8. Chalouhi N, Ali MS, Jabbour PM, et al. **Biology of intracranial aneurysms: role of inflammation.** *J Cereb Blood Flow Metab* 2012;32:1659–76
9. Frosen J, Tulamo R, Heikula T, et al. **Lipid accumulation, lipid oxidation, and low plasma levels of acquired antibodies against oxidized lipids associate with degeneration and rupture of the intracranial aneurysm wall.** *Acta Neuropathol Comm* 2013;1:71
10. Klein IF, Lavallee PC, Mazighi M, et al. **Basilar artery atherosclerotic plaques in paramedian and lacunar pontine infarctions: a high-resolution MRI study.** *Stroke* 2010;41:1405–19
11. Song HK, Wright AC, Wolf RL, et al. **Multislice double inversion pulse sequence for efficient black-blood MRI.** *Magn Reson Med* 2002;47:616–20
12. Kimura T, Ikedo M, Takemoto S. **Hybrid of opposite-contrast MR angiography (HOP-MRA) combining time-of-flight and flow-sensitive black-blood contrasts.** *Magn Reson Med* 2009;62:450–58
13. Tsuchiya K, Kobayashi K, Nitatori T, et al. **Hybrid of opposite-contrast MRA of the brain by combining time-of-flight and black-blood sequences: initial experience in major trunk stenoocclusive diseases.** *J Magn Reson Imaging* 2010;31:56–60
14. Tsuchiya K, Yoshida M, Imai M, et al. **Hybrid of opposite-contrast magnetic resonance angiography of the brain by combining time-of-flight and black blood sequences: its value in Moyamoya disease.** *J Comput Assist Tomogr* 2010;34:242–46
15. Krings T, Piske RL, Lasjaunias PL. **Intracranial arterial aneurysm vasculopathies: targeting the outer vessel wall.** *Neuroradiology* 2005;47:931–37
16. Park JK, Lee CS, Sim KB, et al. **Imaging of the walls of saccular cerebral aneurysms with double inversion recovery black-blood sequence.** *J Magn Reson Imaging* 2009;30:1179–83
17. Matouk CC, Mandell DM, Gunel M, et al. **Vessel wall magnetic resonance imaging identifies the site of rupture in patients with multiple intracranial aneurysms: proof of principle.** *Neurosurgery* 2013;72:492–96
18. Edjlali M, Gentric JC, Regent-Rodriguez C, et al. **Does aneurysmal wall enhancement on vessel wall MRI help to distinguish stable from unstable intracranial aneurysms?** *Stroke* 2014;45:3704–06
19. Hasan DM, Mahaney KB, Magnotta VA, et al. **Macrophage imaging within human cerebral aneurysms wall using ferumoxytol-enhanced MRI: a pilot study.** *Arterioscler Thromb Vasc Biol* 2012;32:1032–38
20. Kleinloog R, Korkmaz E, Zwanenburg JJ, et al. **Visualization of the aneurysm wall: a 7.0 Tesla MRI study.** *Neurosurgery* 2014;75:614–22
21. Kosierkiewicz TA, Factor SM, Dickson DW. **Immunocytochemical studies of atherosclerotic lesions of cerebral berry aneurysms.** *J Neuropathol Exp Neurol* 1994;53:399–406
22. Grigorian AA, Marcovici A, Flamm ES. **Intraoperative factors associated with surgical outcome in patients with unruptured cerebral aneurysms: the experience of a single surgeon.** *J Neurosurg* 2003;99:452–57
23. Szelenyi A, Beck J, Srametz R, et al. **Is the surgical repair of unruptured atherosclerotic aneurysms at a higher risk of intraoperative ischemia?** *Clin Neurol Neurosurg* 2011;113:129–35